Proposal of constitutive models for high-strength concrete reinforced with glass and polymeric fibers

Ricardo Almeida, Guilherme Parsekian, Marco Carnio

Department of Civil Engineering
Federal University of São Carlos
Washington Luís Road – km 235, São Carlos – São Paulo – Brazil
Postal code: 13565-905

Summary

Constitutive models capable of accurately representing the post-cracking behavior of fiber-reinforced concrete are a constant focus of research in the technical literature. However, most of these constitutive models focus exclusively on steel fiber-reinforced concrete, while research on constitutive models of fiber-reinforced high-strength concrete with different fiber types remains scarce. This study investigates the applicability of the constitutive models from the *fib* Model Code 2010 in high-strength concrete reinforced with glass (chopped and pultruded) and polymeric (monofilament and twisted) fibers. A finite element numerical model was developed and validated through an experimental program conducted by the authors. The findings indicate that standardized models do not accurately capture the initial ascending phase for most of the fibers studied, leading to an underestimation of the concrete's toughness in some cases, and new constitutive models were proposed.

1 INTRODUCTION

The primary goal of characterizing the mechanical behavior of materials is to obtain constitutive models – stress-strain curves – that drives the structural response [1]. These constitutive models are essential for structural design. In the context of fiber-reinforced concrete (FRC), the tensile structural response is a main point of interest as fibers primarily contributes under tensile loading.

Identifying the most suitable constitutive model to simulate the post-cracking behavior of fiber-reinforced concrete is key in designing FRC structures [2]. Over the past 20 years, several standards and technical guidelines on the design of FRC structures introduce different constitutive models to simulate post-cracking behavior [3], [4]. The post-cracking behavior of fiber-reinforced concrete is commonly represented by multilinear diagrams due to their simplicity, making them easily applicable in the design of FRC structures.

Constitutive models capable of accurately representing the post-cracking behavior of fiber-reinforced concrete are a constant focus of research in the technical literature. Most of these constitutive models focus exclusively on steel fiber-reinforced concrete, while research on constitutive models of fiber-reinforced high-strength concrete with different fiber types remains scarce. This study investigated the applicability of the constitutive models from the *fib* Model Code 2010 (MC2010) [4] in high-strength concrete reinforced with different fiber types and proposes new design constitutive models through inverse analysis.

2 INVERSE ANALYSIS

Inverse analysis is commonly used to derive stress-strain or stress-crack opening curves under tensile of fiber-reinforced concrete [5]-[9]. This approach is adopted to address the limitations of direct tensile testing, including issues such as specimen misalignment and the need of specialized equipment to fix the specimen to the testing machine [1]. In this study, inverse analysis was employed to propose constitutive models through numerical simulations using the finite element analysis (FEA) with the ABAQUS package. This method aligns with approaches by other researchers such as [10]-[13]. The process for deriving the constitutive model is illustrated in the Figure 1 flowchart. Parameters such as the limit of proportionality (LOP) and residual strengths ($f_{R,j}$) obtained from 3-point bending tests (3PBT) performed according to EN 14651 [14] by the authors [15] served as the basis for defining the input parameters in the numerical model, which correspond to key points in the proposed constitutive model. Numerically generated stress-CMOD (crack mouth opening displacement) curves and their resulted toughness were compared to experimental curves. If the discrepancy between the two was less than 10%, the numerical model was validated, and a constitutive relationship was established. If not, the constitutive model was refined, and the analysis was repeated. This iterative process continued until the toughness difference resulted below the 10%.

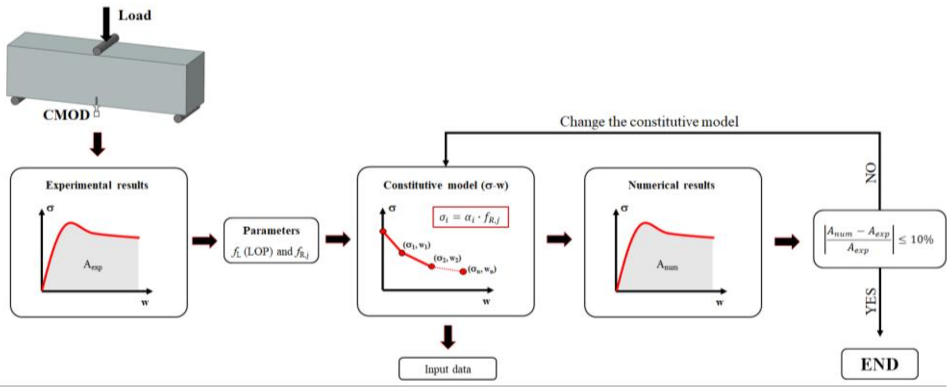

Fig. 1 Inverse analysis procedure

The experimental campaign included two types of glass fibers (chopped – CHGL – and pultruded – PUGL) and two types of polymeric fibers (monofilament – MOPO – and twisted – TWPO) (Figure 2), each studied at three different volume fractions (0.50%, 0.75% and 1.00%). The tensile strength and elastic modulus of the fibers are presented in Table 1 [15].

Table 1 Tensile strength and elastic modulus of the fibers.

Mechanical property	Chopped glass fiber	Pultruded glass fiber	Monofilament polymeric fiber	Twisted polymeric fiber
Tensile strength [MPa]	~1000–1700	~800-1000	550	~600-650
Elastic modulus [GPa]	72	~40-45	8.5	9.5

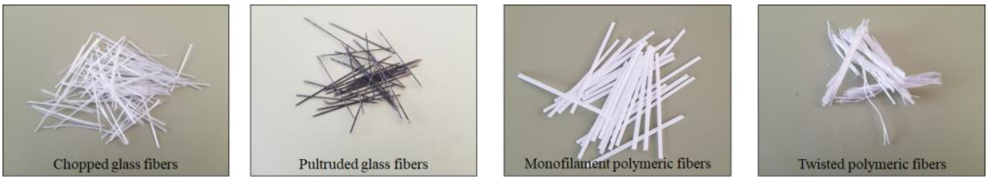

Fig. 2 Fibers used in the analysis.

3 THE NUMERICAL MODEL

The numerical model was developed based on experimental bending test results [15] and its dimensions and boundary conditions were defined according to EN 14651 [14]. Due to the double symmetry, only a quarter of the specimen was modelled to reduce processing time and cost. Symmetry conditions were applied along the XY and YZ planes, and displacement was imposed at the center of the span along the y-axis (Figure 3). The CMOD was measured at the notch near the bottom face of the specimen.

The prism was modelled using eight-node solid elements with reduced integration (C3D8R element from the ABAQUS library) suitable for explicit dynamic analysis [16]. The element front dimensions ranged from 2.50 mm in the notch region to 10 mm in more distant areas, as illustrated in Figure 3. In the transverse direction of the prism axis, the element size was set to 2.50 mm.

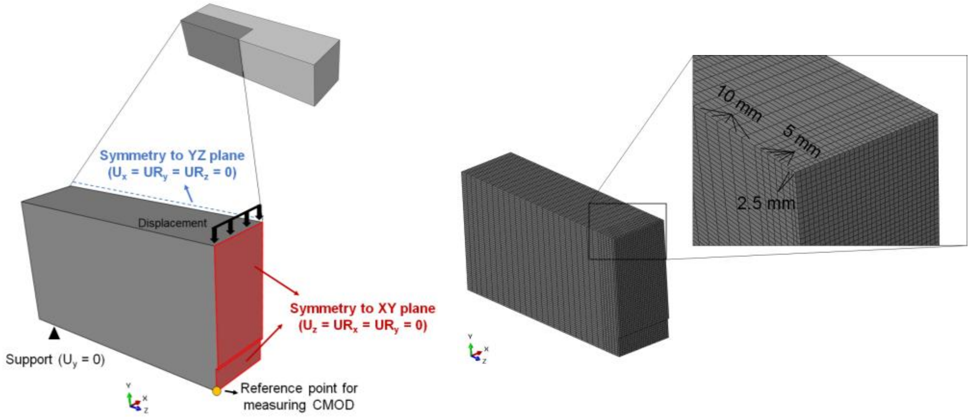

Fig. 3 Numerical model: boundary conditions and finite element mesh

The numerical simulations were carried out using an explicit dynamic analysis due convergence issues. Unlike traditional numerical methods such as Newton-Raphson, explicit analysis is based on dynamic equilibrium, where the global mass and stiffness matrices do not need to be allocated or inverted, resulting in lower computational effort compared to implicit analysis [17]. This type of analysis is typically used to model so-called "quasi-static" events, where the applied loading rate is sufficiently low to make inertia forces negligible. It has been successfully employed by other researchers to study the behavior of fiber-reinforced concrete [11], [18]. To further reduce inertia forces, displacement was applied following a smooth step function, in which ABAQUS generates a fifth-order polynomial transition between two extreme values, ensuring that the first and second derivatives are zero at the beginning and end of the transition. The imposed displacement rate was 0.004 mm/s, closely matching the actual rate used in the experiments.

The nonlinear behavior of concrete was simulated using the Concrete Damaged Plasticity (CDP) model widely used by various researchers to study the mechanical behavior of concrete, including fiber-reinforced concrete [10]-[13]. It accounts for both plastic deformation and damage mechanisms, such as tensile cracking and compressive crushing. The CDP model is defined by the following key parameters: dilation angle (ψ); eccentricity (ε); σ_{b0}/σ_{c0} (biaxial-to-uniaxial strength ratio); K (shape factor); and viscosity parameter (μ). The value of dilation angle (ψ) varied depending on the fiber material (glass and polymeric) while default values were used for the other parameters (Table 2). This is because the dilation angle influences crack propagation in fiber-reinforced concrete beams, with a higher angle leading to more ductile behavior, as observed in glass fiber specimens. Tensile damage (d_t) variables that represents stiffness degradation due to cracking was estimated using equation (1), where σ_t and f_{ctm} represents the tensile stress and the mean tensile strength of the concrete, respectively.

Table 2 Concrete damaged plasticity parameters for numerical simulations

Type of fiber	Concrete Damaged Plasticity				
	ψ	ϵ	f_{b0}/f_{c0}	K	μ
Glass fiber	33º	0.10	1.16	0.67	0.0001
Polymeric fiber	30º	0.10	1.16	0.67	0.0001

$$d_t = 1 - \frac{\sigma_t}{f_{ctm}} \tag{1}$$

The tensile behavior of concrete was simulated using three constitutive models: the rigid-plastic and linear models presented in the MC2010, and the proposed constitutive model. These models consist of multi-linear stress-crack opening diagrams, as illustrated in Figure 4.

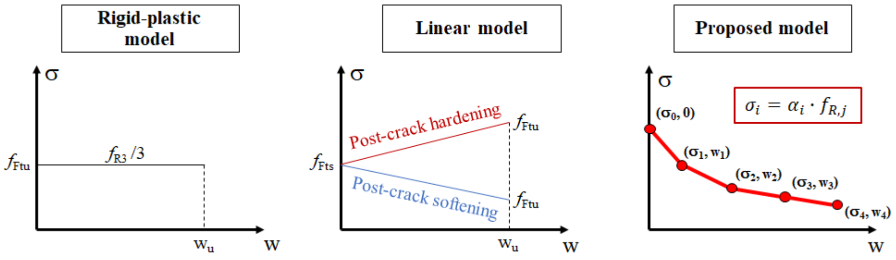

Fig. 4 Constitutive models used in numerical simulations

In the proposed model, the stresses are obtained from the residual strengths ($f_{R,j}$) determined in the bending tests, and the 'w' values correspond to the respective CMODi, except for f_{R1}.

4 RESULTS AND DISCUSSION

The stress-CMOD curves obtained from the numerical simulations are presented in Figure 5 for glass fibers and Figure 6 for polymeric fibers. The curves indicate that only the pultruded glass fiber-reinforced concrete exhibits a strong correlation with the simplified rigid-plastic model from the MC2010. Table 3 presents the toughness values derived from numerical modeling using the three analyzed constitutive models: rigid-plastic, linear, and the proposed model. The error reported was calculated relative to the experimental toughness, following equation (2). Toughness was determined as the area under the curve up to $CMOD_3$ = 2.5 mm associated with the ultimate limit state according to MC2010.

$$Error = \left| \frac{A_{exp} - A_{num}}{A_{exp}} \right| \cdot 100 \tag{2}$$

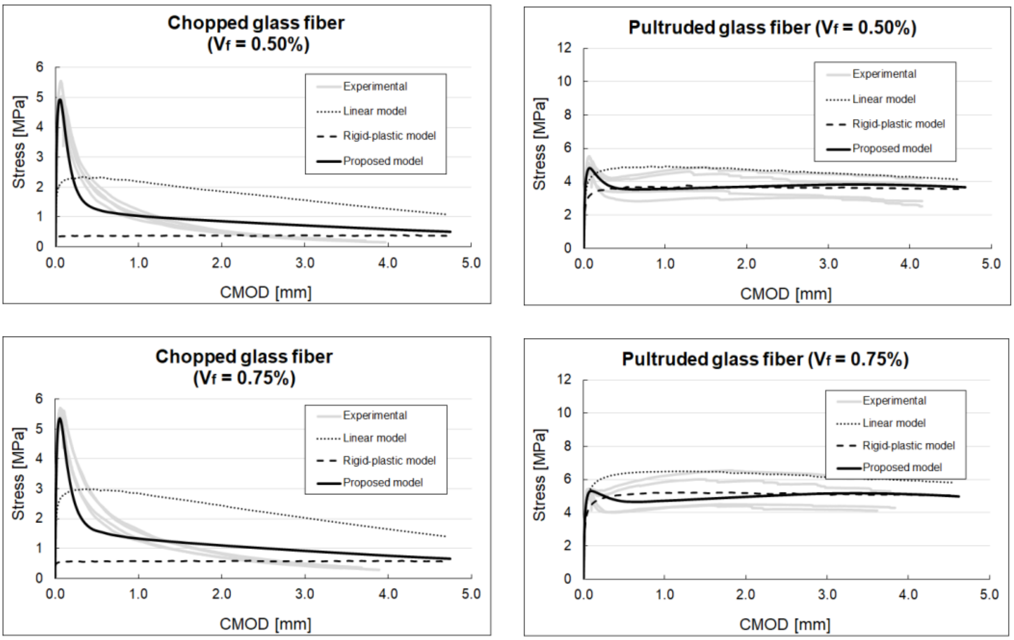

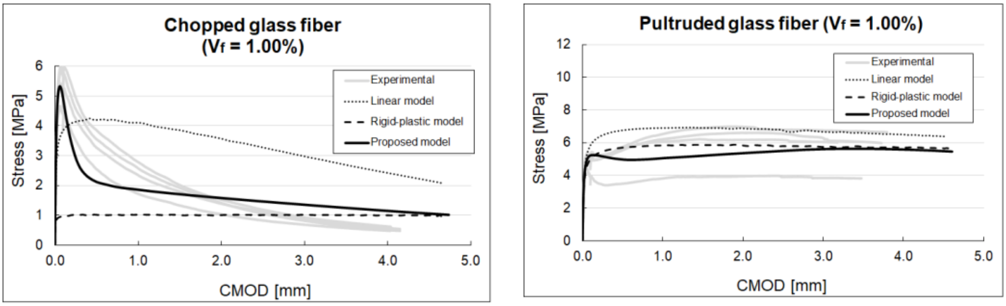

Fig. 5 Results of numerical simulations: glass fibers

For the mixes containing chopped glass fibers, the rigid-plastic and linear constitutive models overestimated the material's toughness by an average of 55% and 85%, respectively, when compared to the experimental results. For both types of polymeric fiber-reinforced concrete, the constitutive models from the MC2010 aligned well only after the load drop observed when the proportionality limit was reached. These standardized models fail to capture the initial ascending phase leading up to the proportionality limit in polymeric fiber mixes, resulting in eventually underestimating the concrete's toughness.

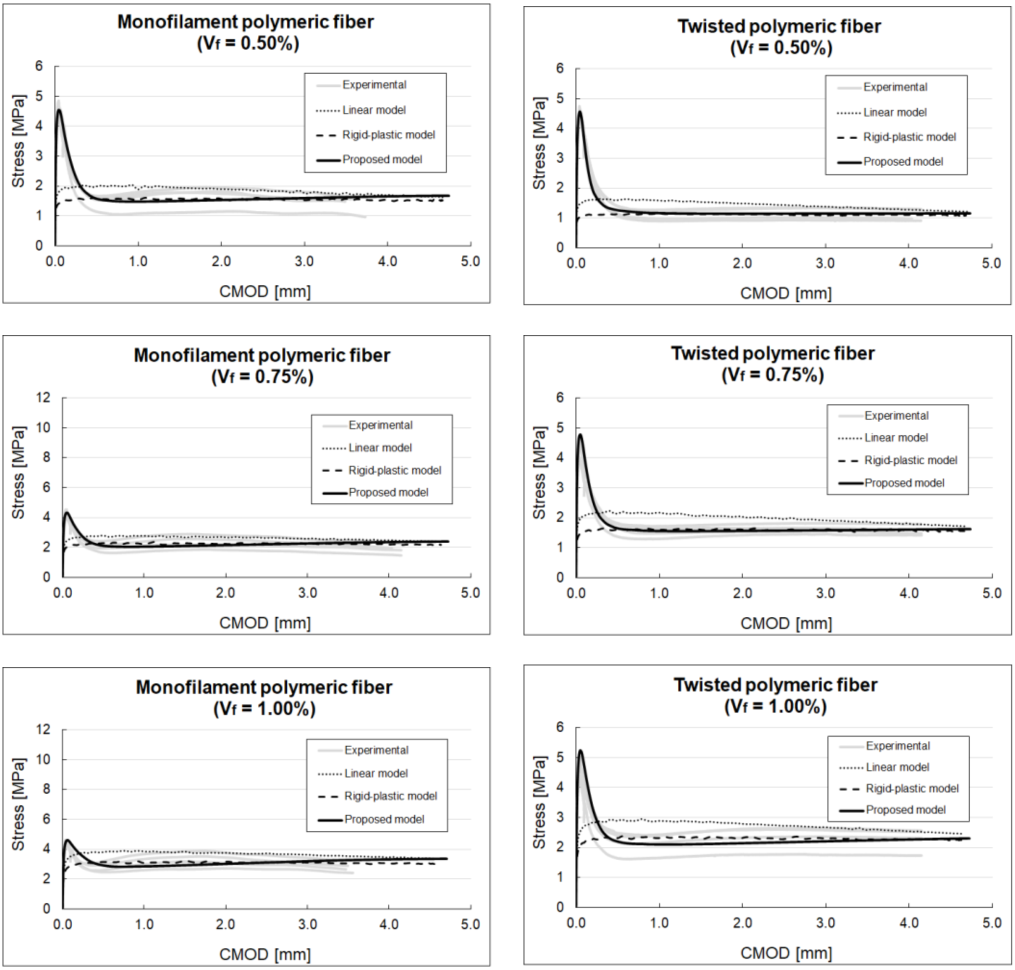

Fig. 6 Results of numerical simulations: polymeric fibers.

The linear model overestimated the concrete's toughness (with errors greater than 10%) for all investigated mixes, while the rigid-plastic model underestimated the toughness of mixes with chopped glass fibers. These inaccuracies could lead to unreliable structural design. These findings suggest that the constitutive models from the technical standard are not suitable to all fiber-reinforced concrete cases studied in this research.

The proposed model exhibited strong agreement with the experimental results across all fiber types and the three studied volume fractions. The model successfully captured the load drop occurring after the proportionality limit was reached. Figure 7 illustrates the cracking patterns observed in both the experimental tests and the numerical model using the damage variable.

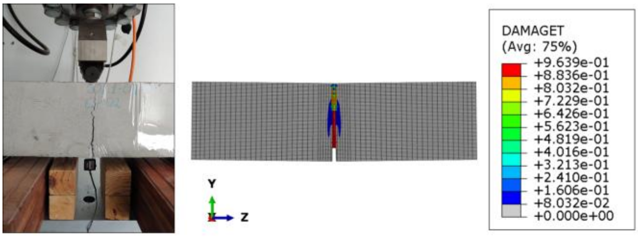

Fig. 7 Experimental and numerical cracking pattern.

Table 3 Toughness provided by different constitutive models

Mix	A_{exp} [N/mm]	$A_{num,RP}$ [N/mm]	Error	$A_{num,linear}$ [N/mm]	Error	$A_{num,proposed}$ [N/mm]	Error
CHGL-0.50	3.66	1.32	63.9%	6.74	84.4%	3.90	6.6%
CHGL-0.75	4.70	2.04	56.7%	8.84	88.2%	4.87	3.6%
CHGL-1.00	6.75	3.55	47.4%	12.69	87.9%	6.49	3.9%
PUGL-0.50	13.28	12.91	2.8%	16.66	25.4%	13.31	0.2%
PUGL-0.75	17.86	18.15	1.6%	22.11	23.8%	17.30	3.2%
PUGL-1.00	19.67	20.26	3.1%	23.58	19.9%	18.89	3.9%
MOPO-0.50	5.96	5.56	6.7%	6.77	13.6%	6.02	1.1%
MOPO-0.75	8.07	7.97	1.3%	9.46	17.2%	8.04	0.4%
MOPO-1.00	10.94	10.86	0.8%	13.19	20.5%	10.94	0.0%
TWPO-0.50	4.60	3.92	15.0%	5.25	14.1%	4.62	0.3%
TWPO-0.75	6.08	5.71	6.0%	7.14	17.5%	6.13	0.8%
TWPO-1.00	8.31	8.18	1.5%	9.85	18.6%	8.16	1.8%

Notes:

A_{exp}: experimental toughness

$A_{num,RP}$: numerical toughness corresponding to rigid-plastic model

$A_{num,linear}$: numerical toughness corresponding to linear model

$A_{num,proposed}$: numerical toughness corresponding to proposed model

The errors associated with the proposed constitutive model remained below 10%. The smallest discrepancies were found in mixes with polymeric fibers, with deviations of less than 2%, while the largest errors occurred in mixes reinforced with chopped glass fibers. Overall, the numerical model effectively replicated the fiber-reinforced concrete behavior observed in the experiments.

5 CONSTITUTIVE MODELS

The constitutive models outlined in the MC2010 are not well-suited for high-strength concrete reinforced with different fiber types, as the numerical toughness obtained using these models deviated significantly from the experimental results. Representative constitutive models here proposed could accurately capture the post-cracking behavior of high-strength fiber-reinforced concrete.

The validation of the numerical model suggests that the tensile constitutive model for FRC should be tailored to the specific type of fiber used as reinforcement. The proposed constitutive models are shown in Figure 8, alongside the rigid-plastic and linear models for comparison purposes.

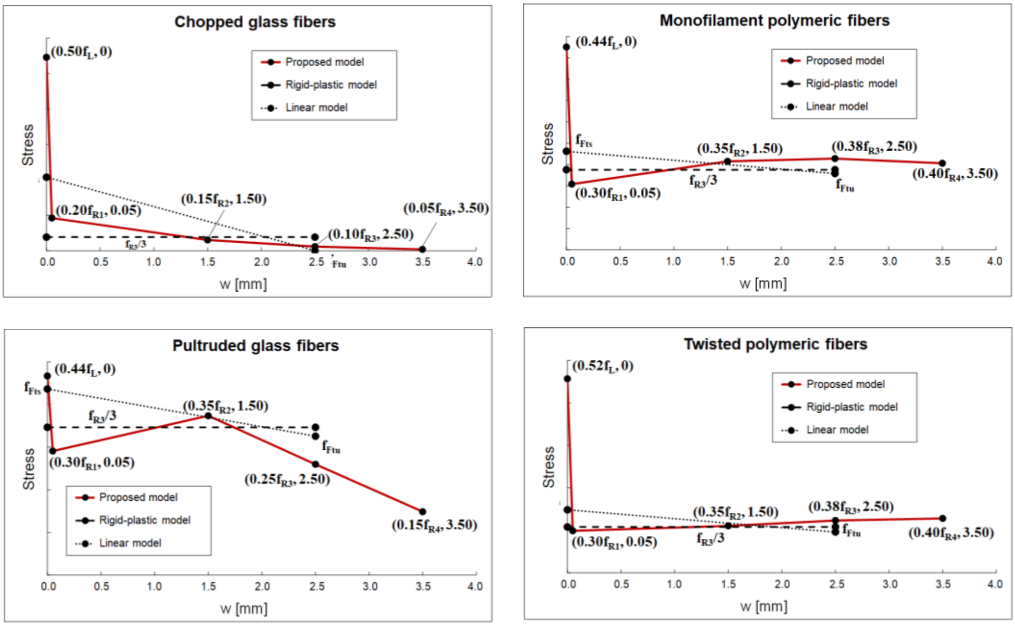

Fig. 8 Proposed constitutive models.

6 CONCLUSIONS

This paper reports the development of a finite element numerical models designed to derive stress-crack opening curve through inverse analysis for high-strength fiber-reinforced concrete. The proposed numerical model was validated against experimental test results.

The difference between the experimentally measured toughness and the values predicted by the numerical model were below 10%. Constitutive models were assessed for concrete reinforced with chopped and pultruded glass fibers, monofilament and twisted polymeric fibers. Three different models were considered: the rigid-plastic and the linear models presented in the MC2010, and a new proposed constitutive model. The linear model consistently overestimated toughness across all analyzed mixes, while the rigid-plastic model provided toughness values close to experimental results for polymeric fibers. Both MC2010 models were unable to capture the post-cracking behavior of fiber-reinforced concrete with this type of fiber. The new proposed constitutive models demonstrated excellent agreement with the experimental results of the high-strength fiber-reinforced concretes evaluated in this study.

At the time of publication of this article, the Model Code 2020 had already been published, introducing significant advancements over Model Code 2010 (MC 2010) in the design and performance-based prescriptions for fiber-reinforced concrete (FRC). These differences reflect the increasing use of FRC in structural applications and the need for more precise design methodologies.

Acknowledgements

Authors wishing to acknowledge the material suppliers: Fabio Saraó, Belgo Bekaert, Matcon Supply, VIAPOL, Owens Corning, MC-Bauchemie and Elkem and Evolução Engenharia for their support in the experiments. This research was funded by the Coordination for the Improvement of Higher Education Personnel (Finance Code 001).

References

[1] T. E. T. Buttignol, J. F. Fernandes, T. N. Bittencourt, and J. L. A. O. Sousa, "Design of reinforced concrete beams with steel fibers in the ultimate limit state," Revista IBRACON de Estruturas e Materiais, vol. 11, no. 5, pp. 997–1024, 2018, doi: 10.1590/s1983-41952018000500006.

[2] A. Blanco, P. Pujadas, A. De La Fuente, S. Cavalaro, and A. Aguado, "Application of constitutive models in European codes to RC-FRC," Constr Build Mater, vol. 40, pp. 246–259, 2013, doi: 10.1016/j.conbuildmat.2012.09.096.

[3] L. Vandewalle, "Test and design methods for steel fibre reinforced concrete," Materials and Structures/Materiaux et Constructions, vol. 36, no. 262, pp. 560–567, 2003, doi: 10.1617/14007.

[4] International Federation for Structural Concrete, "fib Model Code for concrete structures 2010," 2013, Verlag Ernst & John, Berlin.

[5] G. Blasi and M. Leone, "Inverse analysis-based model for the tensile behaviour of fibre-reinforced concrete with manufactured and waste tyres recovered fibres," Case Studies in Construction Materials, vol. 17, no. June, p. e01297, 2022, doi: 10.1016/j.cscm.2022.e01297.

[6] D. Gao, C. Ding, Y. Pang, and G. Chen, "An inverse analysis method for multi-linear tensile stress-crack opening relationship of 3D/4D/5D steel fiber reinforced concrete," Constr Build Mater, vol. 309, no. 97, p. 125074, 2021, doi: 10.1016/j.conbuildmat.2021.125074.

[7] Y. Q. Guo, J. Y. Wang, and J. Ben Gu, "Nonlinear Inverse Analysis for Predicting the Tensile Properties of Strain-Softening and Strain-Hardening UHPFRC," Materials, vol. 15, no. 9, pp. 1–20, 2022, doi: 10.3390/ma15093067.

[8] B. Mobasher, M. Bakhshi, and C. Barsby, "Backcalculation of residual tensile strength of regular and high performance fiber reinforced concrete from flexural tests," Constr Build Mater, vol. 70, pp. 243–253, 2014, doi: 10.1016/j.conbuildmat.2014.07.037.

[9] S. J. Stephen, B. Raphael, R. Gettu, and S. Jose, "Determination of the tensile constitutive relations of fiber reinforced concrete using inverse analysis," Constr Build Mater, vol. 195, pp. 405–414, 2019, doi: 10.1016/j.conbuildmat.2018.11.014.

[10] W. Abbass and M. Iqbal Khan, "Experimental and numerical investigation of flexural behavior of hybrid fiber reinforced high strength incorporating binary and ternary blend of ultra fines," Structures, vol. 42, no. June, pp. 53–64, 2022, doi: 10.1016/j.istruc.2022.05.116.

[11] A. A. Abdulhameed et al., "The Behavior of Hybrid Fiber-Reinforced Concrete Elements: A New Stress-Strain Model Using an Evolutionary Approach," Applied Sciences (Switzerland), vol. 12, no. 4, 2022, doi: 10.3390/app12042245.

[12] M. Alhassan, N. Betoush, N. Al-Huthaifi, and A. Al Dalou, "Estimation of the fracture parameters of macro fiber-reinforced concrete based on nonlinear elastic fracture mechanics simulations," Results in Engineering, vol. 15, no. June, p. 100539, 2022, doi: 10.1016/j.rineng.2022.100539.

[13] C. Lakavath, S. Suriya Prakash, and S. Dirar, "Experimental and numerical studies on shear behaviour of macro-synthetic fibre reinforced prestressed concrete beams," Constr Build Mater, vol. 291, p. 123313, 2021, doi: 10.1016/j.conbuildmat.2021.123313.

[14] European Committee for Standardization, "EN 14651: Test method for metallic fiber-reinforced concrete – Measuring the flexural tensile strength (limite of proporcionality (LOP), residual)," 2007.

[15] R. L. J. de Almeida, G. A. Parsekian, and M. A. Carnio, "Investigation on the flexural behavior of high-strength fiber-reinforced concrete," Structural Concrete, Aug. 2024, doi: 10.1002/suco.202301031.

[16] SIMULIA, "ABAQUS analysis user's manual," 2012, Providence.

[17] R. L. J. de Almeida et al., "Assessing the bearing capacity of Crestbond shear connectors to concrete pry-out," Revista IBRACON de Estruturas e Materiais, vol. 16, no. 1, pp. 1–19, 2023, doi: 10.1590/s1983-41952023000100007.

[18] W. S. A. Nana et al., "Behaviour of macro-synthetic fibers reinforced concrete: Experimental, numerical and design code investigations," Structures, vol. 32, no. December 2020, pp. 1271–1286, 2021, doi: 10.1016/j.istruc.2021.03.080.